A Morphological Study of a Semicrystalline Poly(L-lactic acid-*b*-ethylene oxide-*b*-L-lactic acid) Triblock Copolymer

Dongseok Shin, Kyusoon Shin, Khaled A. Aamer, Gregory N. Tew, and Thomas P. Russell*

Department of Polymer Science and Engineering, University of Massachusetts at Amherst, Amherst, Massachusetts 01003

Jun Hyup Lee and Jae Young Jho

School of Chemical Engineering and Hyperstructured Organic Materials Research Center, Seoul National University, Kwanak, Seoul 151-744, Korea

Received September 7, 2004; Revised Manuscript Received October 21, 2004

ABSTRACT: Poly(L-lactic acid-*b*-ethylene oxide-*b*-L-lactic acid) (PLLA-*b*-PEO-*b*-PLLA) triblock copolymers were synthesized by a ring-opening polymerization. PLLA and PEO sequentially crystallized by slowly cooling (−2 °C/min) from the melt. In the resultant spherulitic morphology, the retardation of polarized light was additive, and the sign of the spherulite (negative) was preserved when the PEO crystallized within the framework established by the PLLA crystals. Homopolymer blends of PLLA and PEO having the same composition as the block copolymer showed similar optical behavior. However, the change in the optical retardation upon crystallization of the PEO was much greater for the triblock copolymer than for the blend. Upon heating, the small-angle X-ray scattering from both the triblock copolymer and homopolymer mixture showed a stepwise increase in the long period at ∼60 °C, i.e., when the PEO crystals melted. For comparable volume fractions ($\phi_{PLLA} = 0.57$), the increase in long period was greater for the triblock copolymer than for the blend. Wide-angle X-ray diffraction studies on shear aligned triblock copolymers indicate that the PLLA and PEO crystals adopt the same average orientation; though, in the case of the copolymer, the orientation is more strongly coupled.

Introduction

By covalently linking dissimilar polymer chains in a block copolymer, the immiscibility of the blocks results in a microphase separation of the components, where the volume fractions and molecular weights of each block dictate the type and size of the microdomains.[1] In cases where one of the blocks can crystallize, the microdomain morphology provides a unique opportunity to investigate crystallization in confined geometries.[2] The ultimate morphology formed with a crystalline−amorphous block copolymer depends on the relative location of the order−disorder transition temperature (T_{ODT}), the glass transition temperature (T_g) of the amorphous block, and the crystallization temperature (T_c) of the semicrystalline block.[3] If $T_{ODT} > T_g > T_c$, then the crystallization occurs within the confines of the microdomains bounded by the second glassy component. If $T_{ODT} > T_c > T_g$, crystallization occurs within the microdomains, but the second component is above its T_g, i.e., rubbery, then the crystals can protrude into the rubbery domain. If $T_{ODT} < T_c > T_g$, then crystallization takes place in the phase mixed state, and microphase separation is driven by crystallization which leads to a lamellar morphology regardless of the composition. In both the hard confinement[2] ($T_{ODT} > T_g > T_c$) and soft confinement ($T_{ODT} > T_c > T_g$) cases,[4,5] the orientation of the crystals, with respect to the microphase interface, has been investigated. However, studies on crystalline−crystalline block copolymers have been discussed to a much lesser extent. Misra et al.[6] and Albuerne et al.[3] reported that crystals of the faster crystallizing block functioned as nucleation sites for the second block. Lee et al.[7] investigated the chain length effect of one block on the crystallization of the other, using poly(L-lactic acid)−poly(ethylene oxide) multiblock copolymers. Although some groups have begun to study crystalline−crystalline block copolymers,[3,6−12] the morphological understanding of such materials is still in its nascent stage.

Here, poly(L-lactic acid-*b*-ethylene oxide-*b*-L-lactic acid) (PLLA-*b*-PEO-*b*-PLLA) triblock copolymers were investigated. PLLA is a biodegradable polymer, whereas PEO is biocompatible. As such, these materials represent interesting candidates for environmentally friendly packaging materials[13] and biomedical applications.[14] PEO and PLLA are reported to be miscible in the melt[15] and PEO does not cocrystallize with PLA.[16] In addition, the difference between the melting temperatures of PLLA (145−186 °C)[17] and PEO (66 °C)[17] enables an investigation of the sequential crystallization of the components. In this work, PLLA and PEO blocks were sequentially crystallized by slowly cooling from the melt. The morphology was investigated as a function of temperature using polarized optical microscopy, differential scanning calorimetry, and wide- and small-angle X-ray scattering. In addition, homopolymer mixtures of PEO and PLLA were examined for comparison to the triblock copolymer.

Experimental Section

PLLA-*b*-PEO-*b*-PLLA triblock copolymers were synthesized by a ring-opening polymerization.[18] L-Lactide (Aldrich) was purified by recrystallization in dry ethyl acetate and sublimed prior to polymerization. The α,ω-dihydroxypoly(ethylene glycol) (PEG) macroinitiators with molecular weights of 12K, 35K (Alfa Aesar), and 20K (Avocado) were dried at room temperature under vacuum prior to polymerization. Stannous(II) 2-ethylhexanoate (Alfa Aesar) was used without further purification. Bulk polymerization was performed to synthesize triblock copolymers. In a typical polymerization, PEG was introduced into a dried polymerization tube. The tube was

10.1021/ma0481712 CCC: $30.25
Published on Web 12/07/2004

Table 1. Characteristics of Triblock Copolymer Employed

samples	M_n[a]	PDI[b]	ϕ_{PLLA}
$PLLA_{33}-PEO_{795}-PLLA_{33}$[c]	39 800	1.09	0.11
$PLLA_{209}-PEO_{455}-PLLA_{209}$	50 100	1.17	0.57
$PLLA_{136}-PEO_{273}-PLLA_{136}$	31 600	1.20	0.59
$PLLA_{269}-PEO_{273}-PLLA_{269}$	50 800	1.12	0.74

[a] Value determined from ^{1}H NMR integration between the methine proton of PLLA and the methylene protons of PEO. [b] Value measured from SEC. [c] Subscript numbers represent the degree of polymerization.

purged with nitrogen and placed in an oil bath at 150 ± 1 °C. Stannous(II) 2-ethylhexanoate was introduced under nitrogen to the molten PEG and stirred for 10 min, followed by the addition of L-lactide to the macroinitiator/catalyst melt. The polymerization was carried out for 24 h with stirring, after which it was quenched by methanol. The product was dissolved in tetrahydrofuran and precipitated in *n*-hexane. The process of dissolution/reprecipitation was carried out three more times. The triblock copolymer was dried under vacuum at room temperature for 2 days.

The molecular weights and compositions of the triblock copolymers were determined by ^{1}H NMR (Bruker, DPX300, 300 MHz spectrometer, d-chloroform). Molecular weights and polydispersities were measured against polystyrene standards using size exclusion chromatography (Waters 600, equipped with a Waters 410 differential refractometer, a Waters 717 pluse autosampler, and three PLgel columns, 5 mm Mixed-D). Chloroform was used as the eluting solvent at a rate of 1.0 mL/min, and measurements were performed at room temperature. The characteristics of the triblock copolymers used in this study are summarized in Table 1. The volume fractions were calculated using the amorphous densities of 1.123 g/cm^3 for PEO[19] and 1.248 g/cm^3 for PLLA.[17]

Homopolymer blends of PLLA and PEO were also investigated. Homopolymers were purchased from commercial sources, PEO (M_w = 39 000 g/mol, PDI = 1.07, Polymer Laboratory) and PLLA (M_w = 22 200 g/mol, PDI = 1.30, Polymer Source). They were used without further purification. The blends were cast from 5% (w/v) chloroform solutions. After evaporating the solvent at ambient conditions, the remaining solvent was removed under vacuum at 170 °C for 30 min.

For the optical studies, polymers were melt-pressed between two optical microscope coverslips (150 μm thick). Samples were heated to 190 °C and held at that temperature for 3 min to erase any thermal history. They were then slowly cooled (−2 °C/min) to room temperature. The final thickness of the polymer film was in the range 10−20 μm. The optical properties of the samples were measured using a polarized optical microscope (Olympus BX-60) under cross-polar conditions. The temperature of the sample was controlled with a hot stage (Mettler FP82). The sign of the birefringence was determined using a first-order red plate (λ = 530 nm), and the magnitude of optical retardation was measured using a Berek compensator (U-CBE). The compensator was inserted between the sample and the analyzer at an angle of 45° relative to both polarizer and analyzer.

The thermal behavior of a melt-crystallized sample was investigated by differential scanning calorimetry (DSX 2910 of DuPont Instrument) under a nitrogen gas flow (50 cm^3/min). The heating rate was set at 10 °C/min. The samples for DSC experiments were prepared using hermetically sealed Al pans and thermally treated as described above. The melting enthalpies (ΔH_f) obtained from the thermograms were used to calculate the crystallinities of the components based on the reported heats of fusion ($\Delta H_f°$) of 197 J/g for PEO and 94 J/g for PLLA.[20]

Small-angle and wide-angle X-ray diffraction studies were performed using an instrument from the Molecular Metrology Inc., equipped with a focusing multilayer monochromator (Osmic MaxFlux) with λ = 1.54 Å. The beam was collimated with three pinholes. For the small angle detection, a 2-D multiwire detector (sample-to-detector distance of 1.5 m) was used. To record the wide angle profiles, an image plate with a hole in the center was inserted into the beam path. The sample was pressed between Kapton films (50 μm thick) and thermally treated as described above. Samples were heated to 190 °C for 10 min and then cooled to room temperature at the rate of −2 °C/min. For the wide-angle diffraction studies, the scattering peak of Kapton at $q = 4\pi \sin\theta/\lambda = 0.41$ Å^{-1} was used as an internal standard and a $CaCO_3$ standard (d_{111} = 3.035 Å) was used for angular calibration. Silver behenate (d_{001} = 58.38 Å) was used for angular calibration of the SAXS measurements.

Samples were aligned in a shearing hot stage (CSS 450 Linkam Scientific Instruments). A disk-shaped sample of the triblock copolymer (ϕ_{PLLA} = 0.57) was held between concentric disks and heated to 180 °C. The gap distance was set at 500 μm, and a shear (shear rate = 30 s^{-1}) was applied. After 5 min, the samples were cooled at the rate of −30 °C/min to 120 °C and held at 120 °C for 4 min. Shear was continuously applied to align the PLLA lamellae. Subsequently, the samples were cooled (−30 °C/min) to 50 °C, removed from the hot stage, and then quenched in liquid nitrogen to preserve the PLLA lamellae orientation. Subsequently, the samples were heated to 80 °C (above the melting temperature of PEO) and then slowly cooled (−2 °C/min) to room temperature.

Results and Discussion

I. Optical Properties. Figure 1 shows optical micrographs taken with identical exposure times but at different temperatures (140, 80, and 25 °C) during cooling. In the melt (190−130 °C), no birefringence was observed for both the triblock copolymers and homopolymer blends. If the block copolymers were microphase separated, a form birefringence would be expected. Consequently, the microscopy results indicate that the copolymer is phase mixed at these temperatures. This result agrees well with the reported miscibility of PLLA and PEO in the amorphous state.[15] Near 125 °C, the nucleation and growth of spherulites were seen over the entire composition and molecular weight ranges studied. Both the triblock copolymers and blends produced banded spherulites. Nojima et al.[21] noted two requirements to produce banded spherulites: (1) the thermodynamic compatibility of the components[22] and (2) specific interactions between the components. Consequently, the observation of banding is consistent with the inclusion of PEO within the interlamellae regions while PLLA crystallizes and the miscibility of the components where specific interactions between the PEO chains and surface of the PLLA crystals would occur.

After the spherulites impinged on one another the optical micrograph did not change upon further cooling until ∼35 °C when the image under crossed polars substantially brightened. This intensification of the image corresponds to the crystallization of PEO, and since the intensity increased, the retardation of the PLLA and PEO crystals must be additive. Furthermore, the sign of the spherulites, determined with a first-order red plate, was conserved. The sign of the spherulites for the triblock copolymers and for PLLA and PEO homopolymers was the same (negative; $n_r < n_t$). Remarkably, during the sequential crystallization of PEO within the framework of the existing PLLA spherulite, the retardation colors, positions of extinction, and widths of the bands remained constant. Only the brightness of the field increased. Even more surprising is that a similar behavior was found for the mixtures of PLLA and PEO homopolymers. Recalling that, in the triblock copolymer, PEO crystallizes under the con-

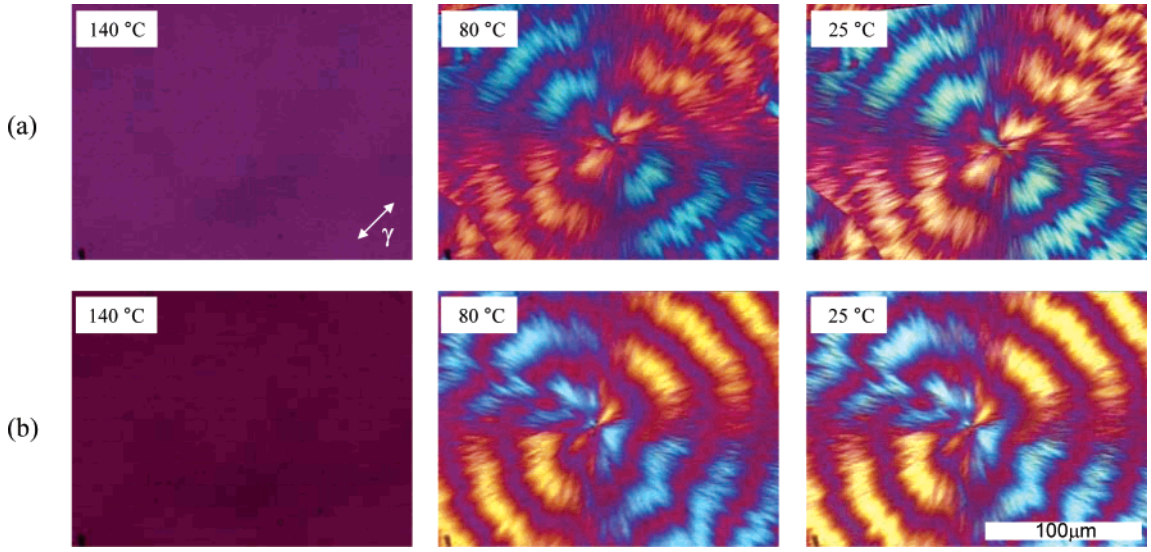

Figure 1. Polarized optical micrographs taken at 140, 80, and 25 °C during a cooling (−2 °C/min) process: (a) $PLLA_{209}$−PEO_{455}−$PLLA_{209}$; (b) PLLA/PEO blend ($\phi_{PLLA} = 0.57$). A first-order red plate ($\lambda = 530$ nm) was inserted in the light path.

Table 2. Optical Retardation Ratio (Room Temperature to 80 °C) of Employed Materials

samples	ϕ_{PLLA}	$R_{RT}/R_{80\ °C}$[a]
$PLLA_{33}$−PEO_{795}−$PLLA_{33}$	0.11	9.478 ± 0.195
$PLLA_{209}$−PEO_{455}−$PLLA_{209}$	0.57	1.351 ± 0.023
$PLLA_{136}$−PEO_{273}−$PLLA_{136}$	0.59	1.346 ± 0.022
$PLLA_{269}$−PEO_{273}−$PLLA_{269}$	0.74	1.143 ± 0.038
PLLA/PEO blend I	0.37	2.049 ± 0.038
PLLA/PEO blend II	0.57	1.270 ± 0.029

[a] Optical retardation (R) was measured five times at each temperature. Errors represent standard deviation.

straint of having both ends of the PEO anchored to the existing PLLA crystals, the similarity of results for the blend and block copolymers is unexpected. It implies that the crystallization of the PEO is strongly templated by the existing crystalline lamellae of PLLA. Upon heating at 2 °C/min, the reverse transitions of sequential melting were observed but at temperatures slightly higher than those seen on cooling. This hysteresis is not unusual with semicrystalline polymers.

The magnitude of birefringence, or more precisely, the optical retardation (R) was measured at room temperature and 80 °C. To eliminate thickness effects, the ratio of the retardation at room temperature (RT) to that at 80 °C ($R_{RT}/R_{80\ °C}$) was determined and compared to calculations. The results are summarized in Table 2, and as could be expected, this ratio increased as the PEO composition increased. Comparing the triblock copolymer and homopolymer blends, the triblocks showed a larger change in the optical retardation than the homopolymer mixtures. Ignoring the form birefringence, the total birefringence, Δ, is given by[23]

$$\Delta = \sum \phi_i f_i \Delta_i^0 \quad (1)$$

where Δ_i^0 is the intrinsic birefringence of component i with a volume fraction ϕ_i and orientation function f_i. For the PLLA-*b*-PEO-*b*-PLLA triblock copolymer, where PEO and PLLA have crystalline and amorphous components, Δ is given by

$$\Delta = \phi_{c,PLLA} f_{c,PLLA} \Delta^0_{c,PLLA} + \phi_{a,PLLA} f_{a,PLLA} \Delta^0_{a,pLLA} + \phi_{c,PEO} f_{c,PEO} \Delta^0_{c,PEO} + \phi_{a,PEO} f_{a,PEO} \Delta^0_{a,PEO} \quad (2)$$

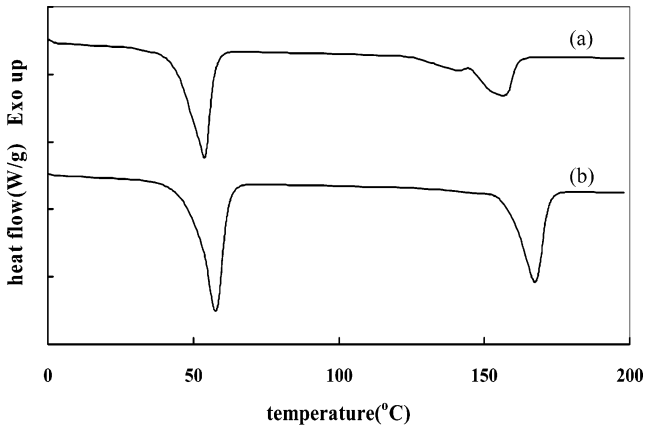

Figure 2. DSC thermograms obtained with a heating rate of 10 °C/min: (a) $PLLA_{209}$−PEO_{455}−$PLLA_{209}$; (b) PLLA/PEO blend ($\phi_{PLLA} = 0.57$). Samples were crystallized by slowly cooling (−2 °C/min) before running DSC.

where "c" and "a" denote the crystalline and amorphous components, respectively. $\phi_{c,PLLA}$ and $\phi_{c,PEO}$ can be determined calorimetrically, and $\phi_{c,i} + \phi_{a,i} = \phi_i$. Since $\Delta^0_{c,i}$ and $\Delta^0_{a,i}$ do not change with crystallization and $f_{a,i} = 0$ (assuming the amorphous components are random), then the enhancement in the intensity must be associated with changes in $\phi_{c,i}$ and/or $f_{c,i}$. Similarly, differences observed between the homopolymer mixtures and block copolymer must be associated with differences in $\phi_{c,i}$ and $f_{c,i}$ of the PEO and PLLA due to the covalent coupling of the two chains.

II. Thermal Behavior. The DSC thermograms of a triblock copolymer and homopolymer blend with comparable compositions ($\phi_{PLLA} = 0.57$) are shown in Figure 2. The triblock copolymer shows a PEO melting peak at ~55 °C and PLLA melting at ~160 °C. A melting point depression for both PEO and PLLA of ~6 °C for both the mixtures and triblock copolymer was observed in comparison to the melting points of the pure homopolymers ($T_{m,PEO} = 60$ °C and $T_{m,PLLA} = 174$ °C), which further supports the conclusion that PEO and PLLA are miscible in the amorphous state.[15] The lower temperature shoulder of the PLLA melting peak of the triblock can be attributed to a melting/recrystallization or lamellar reorganization.[15] The blend system showed

Table 3. Crystallinity of a Triblock Copolymer and a Homopolymer Blend

	triblock copolymer		homopolymer blend	
	PLLA	PEO	PLLA	PEO
ϕ_i	0.57	0.43	0.57	0.43
w_i	0.6	0.4	0.6	0.4
$\Delta H_{f,i}$ (J/g)[a]	28.4	44.4	39.7	53.0
$\Delta H°_{f,i}$ (J/g)[b]	94	197	94	197
$X_{c,i}$	0.50	0.56	0.70	0.67

[a] From DSC. [b] From ref 20.

similar thermal behavior as that of the block copolymer, though the melting peaks were located at higher temperatures and the peak widths were narrower than the corresponding peaks of the triblock copolymer. The crystallinity of each component ($X_{c,i}$) was calculated using the corresponding melting enthalpy ($\Delta H_{f,i}$) obtained from the thermograms and the weight fraction (w_i). So

$$X_{c,i} = \frac{\Delta H_{f,i}}{w_i \Delta H°_{f,i}} \tag{3}$$

As shown in Table 3, the triblock copolymer had a lower crystallinity for each component, particularly PLLA, than the homopolymer blends. Chain connectivity and the reduction of chain mobility in the triblock copolymer can easily cause the observed decrease in $X_{c,i}$. Combining crystallinities calculated from the thermograms with the optical retardation data, the relative birefringence of PLLA and PEO can be approximated as follows

$$\frac{\Delta_{PLLA}}{\Delta_{PEO}} = \frac{(R_{80\,°C})/(\Delta H_{f,PLLA}/\Delta H°_{f,PLLA})}{(R_{RT} - R_{80\,°C})/(\Delta H_{f,PEO}/\Delta H°_{f,PEO})} \tag{4}$$

where Δ_{PLLA} and Δ_{PEO} are the birefringences of PLLA and PEO, respectively. In this calculation, it was assumed that the crystallinity of PLLA was the same at both temperatures and that the amorphous phase did not contribute to optical retardation, i.e., $f_{a,i} = 0$. For the triblock copolymer ($\phi_{PLLA} = 0.57$), $\Delta_{PLLA}/\Delta_{PEO}$ was calculated to be 2.13 while the value of the blend was the same, within experimental errors, at 2.36.

III. X-ray Studies. Wide-angle X-ray diffraction at 20 and 80 °C was used to obtain information about the crystalline structure of PLLA and PEO. The diffraction profiles consisted of isotropic rings that were circularly averaged to improve the signal-to-noise ratio. The resultant diffraction patterns are shown in Figure 3. The peak positions agreed well with the reported unit cell parameters for PEO (monoclinic, $a = 8.05$ Å, $b = 13.04$ Å, $c = 19.84$ Å, $\beta = 125.4°$)[24] and PLLA (orthorhombic, $a = 10.6$ Å, $b = 6.1$ Å, $c = 28.8$ Å).[25] From these unit cell parameters, the crystalline densities of PEO and PLLA were calculated as 1.23 and 1.29 g/cm^3, respectively. The most intense peak located at $q \sim 1.19$ Å^{-1}, corresponding to the (110) and (200) reflections of PLLA,[26] was observed at both 20 and 80 °C. The intensity of the reflection at $q \sim 1.36$ Å^{-1}, corresponding to the (120) reflection of PEO[2] and the calculated values of the (203) and (113) crystal planes of PLLA, decreased as the temperature increased from 20 to 80 °C. The broad peak located at $q \sim 1.65$ Å^{-1}, reported to be an overlap of (032), ($\bar{1}$32), and ($\bar{2}\bar{1}\bar{2}$) reflections of PEO,[2] was observed only in the 20 °C data. Thus, the melting of PEO at 80 °C could easily be determined from the

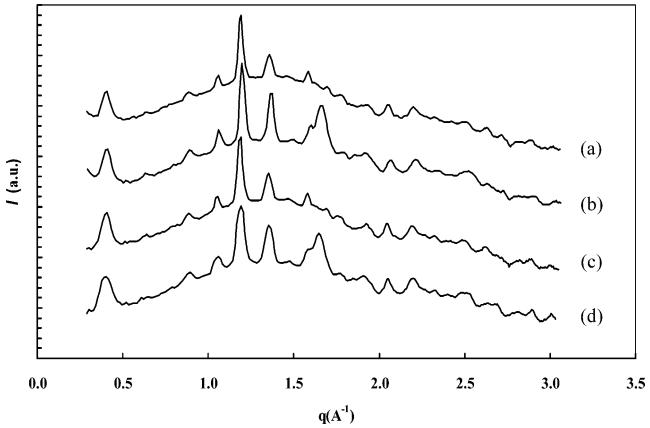

Figure 3. Wide-angle X-ray diffraction patterns measured at 20 °C (b, d) and 80 °C (a,c): (a, b) $PLLA_{209}$−PEO_{455}−$PLLA_{209}$; (c, d) PLLA/PEO blend ($\phi_{PLLA} = 0.57$).

diffraction data. It should be noted that the positions of the crystal reflections did not change with temperature, indicating there were no significant distortions of the crystal structures of PLLA and PEO due to confinement of PEO between the crystalline lamellae of PLLA.

The long period was determined as a function of temperature by in situ small-angle X-ray scattering (SAXS). Scattering profiles of the triblock copolymers and the homopolymer mixtures ($\phi_{PLLA} = 0.57$) were obtained at 20 °C intervals from 20 to 180 °C, allowing 1 h between scans to allow the systems to reach thermal equilibrium. The scattering profiles were Lorentz corrected, $q^2(I - I_{ref})$. SAXS patterns taken at 230 °C for the triblock copolymer and at 210 °C for the homopolymer blend were used to determine the scattering from thermal density fluctuations that was subtracted from each profile. SAXS results for the triblock copolymer and mixture are shown in Figure 4. Between 40 and 80 °C, there was a sharp increase in the long period for both the triblock copolymer and the blend. As shown in Figure 2, this coincides with the melting of the PEO crystals. At 80 °C, the long periods of the triblock copolymer and homopolymer mixture increased by ∼33% and ∼18%, respectively. Since the density of amorphous PEO is ∼1.123 g/cm^3,[19] the volume change accompanying the melting of PEO crystal is ∼9%. This is much less than the observed long period changes, even if, in the extreme case, volume expansion between the lamellae is restricted to being normal to the surface of the PLLA lamellar and confined to the interlamellae regions. If we take thermal expansion into account, the amorphous density of PEO at 80 °C can be estimated at 1.08 g/cm^3.[27] Thus, the volume of PEO increases by ∼14% upon melting, which agrees with the change observed in the long period of the blend but is still smaller than that for the triblock copolymer. On the basis of the crystallinity obtained from the thermograms (Table 3), the amorphous volume fractions of the triblock copolymer and the homopolymer blend at 20 °C were calculated to be 49% and 32%, respectively. This difference corresponds well with the larger change in the long period for the triblock copolymer than in the blend.

For the shear aligned sample, SAXS and WAXD patterns were measured simultaneously and are shown in Figure 5. The X-ray beam path was parallel to the shear gradient direction. From the small-angle scattering pattern, an alignment of the crystalline lamellae in the shear direction was observed. Analysis of the azimuthal dependence of the diffraction patterns was

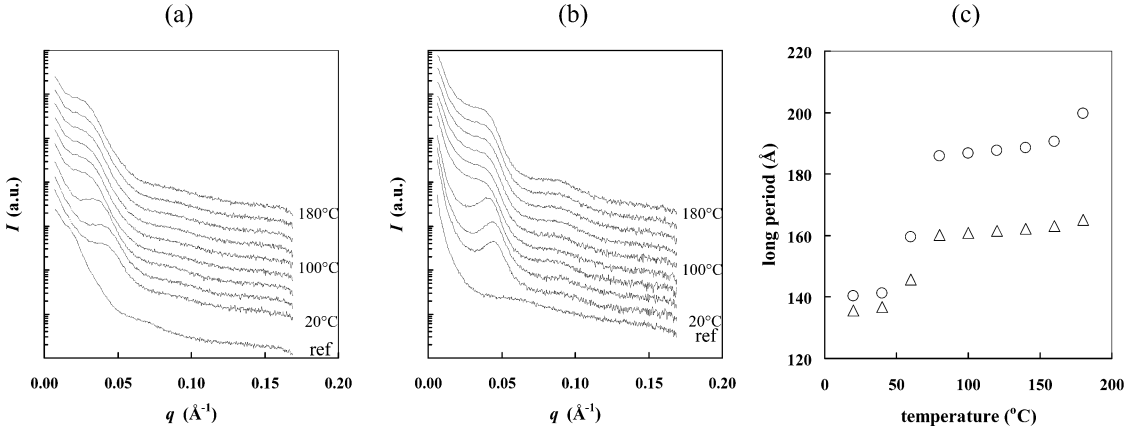

Figure 4. Small-angle X-ray scattering patterns as a function of temperature: (a) $PLLA_{209}-PEO_{455}-PLLA_{209}$, (b) PLLA/PEO blend ($\phi_{PLLA} = 0.57$), and (c) long period vs temperature (○, triblock copolymer; Δ, blend).

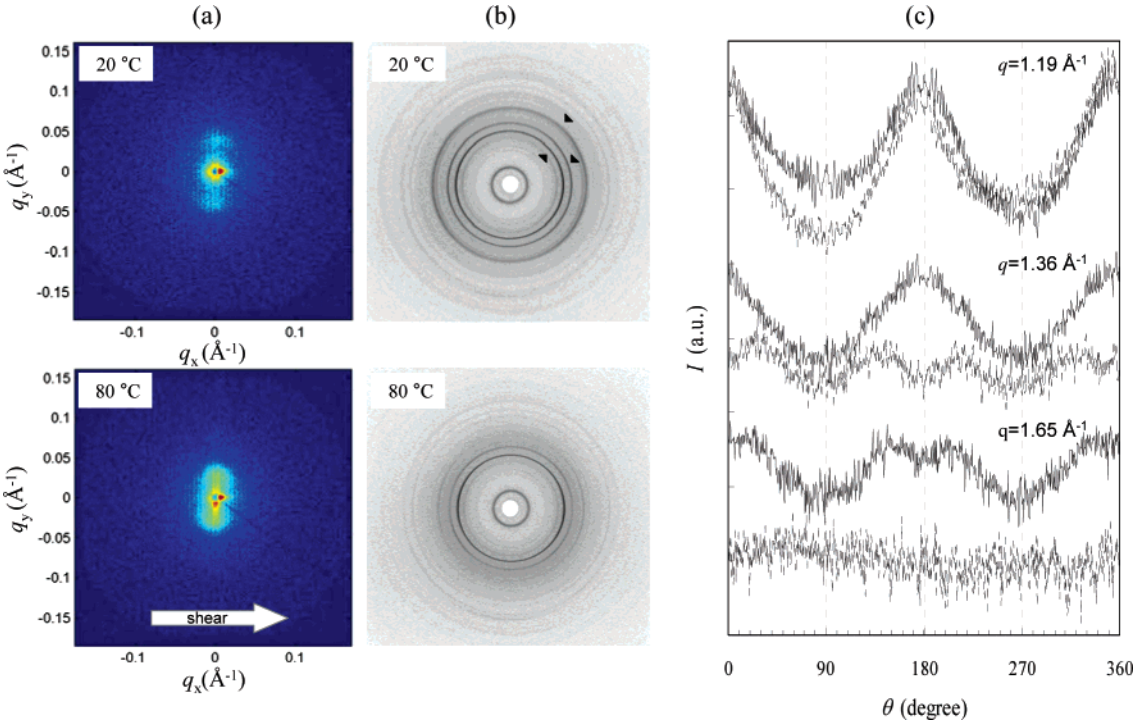

Figure 5. X-ray diffraction patterns of a shear aligned triblock copolymer ($PLLA_{209}-PEO_{455}-PLLA_{209}$) measured at 20 and 80 °C: (a) small angle, (b) wide angle, and (c) azimuthal analysis of wide angle diffraction pattern (—, 20 °C; - - -, 80 °C).

performed on three peaks ($q \sim 1.19$, 1.36, and 1.65 $Å^{-1}$) and is plotted in Figure 5. Even on a qualitative level, comparison of the SAXS and WAXD data shows that the orientation of the crystal axes was much less than that of the lamellae. However, by comparison of these data, in particular the azimuthal dependence of the PLLA (110) reflection ($q \sim 1.19$ $Å^{-1}$ at 20 and 80 °C) and the PEO (120) reflection ($q \sim 1.36$ $Å^{-1}$ at 20 °C), it can be concluded that the PLLA and PEO chain axes in the crystalline phase are both oriented normal to the lamellar surface. This result is consistent with the optical birefringence studies earlier.

From eq 2, it can be deduced that $\phi_{c,i}$ and $f_{c,i}$ give rise to the difference in the optical behavior between the blend and the triblock copolymer. As summarized in Table 3, the triblock copolymer showed a higher relative crystallinity (the ratio of the volume fraction crystallinites of PEO to PLLA). This explains the greater relative retardation of the triblock copolymer to some extent. However, the effect of $f_{c,i}$ cannot be ignored since the anchoring of the PEO chains to the existing PLLA crystals in the triblock copolymer must bias the orientation of the PEO crystals. The relative orientation function of PLLA and PEO chains in the crystalline phase was estimated as following. If we ignore the contribution of amorphous phases to the birefringence and assume that the crystallinity of PLLA does not change between RT and 80 °C, then the ratio of the retardation at room temperature (RT) and at 80 °C can be related to the orientation function of the chain.

$$\frac{R_{RT}}{R_{80\,°C}} \sim \frac{\Delta_{RT}}{\Delta_{80\,°C}} \sim 1 + \frac{\phi_{c,PEO} f_{c,PEO} \Delta^0_{c,PEO}}{\phi_{c,PLLA} f_{c,PLLA} \Delta^0_{c,PLLA}} \qquad (5)$$

Rearranging, the ratio of the orientation function of the PEO and PLLA crystals can be calculated from the following equation.

$$\frac{f_{c,PEO}}{f_{c,PLLA}} \frac{\Delta^0_{c,PEO}}{\Delta^0_{c,PLLA}} = \left(\frac{R_{RT}}{R_{80\,°C}} - 1\right) \frac{\phi_{c,PLLA}}{\phi_{c,PEO}} \qquad (6)$$

Using the data summarized in Tables 2 and 3, this ratio was calculated to be 0.45 for the triblock copolymer ($\phi_{PLLA} = 0.57$) and 0.40 for the blend with the comparable composition. Since the intrinsic birefringences of PEO and PLLA should be the same for the triblock copolymer and for the blend, this result indicates that the PEO crystals in the triblock copolymer have a better relative orientation to PLLA crystals than those in the blend. Thus, the covalent attachment of the PEO to the PLLA crystals in the copolymer must cause the *c*-axes of the PEO crystals to align more closely with the *c*-axes of the PLLA crystals. This, in turn, would lead to a greater increase in the transmitted light intensity, or brightness, under crossed polars for the triblock copolymers.

Conclusion

The morphology of PLLA-*b*-PEO-*b*-PLLA triblock copolymers, comprised of semicrystalline blocks, was investigated. When slowly cooled (−2 °C/min) from a homogeneous melt, a sequential crystallization of PLLA and PEO occurs. During this process, the retardation of the components were additive and the sign of the spherulites (negative, $n_r < n_t$) was conserved. A homopolymer blend with a comparable composition to that of the triblock copolymer showed similar optical behavior, though the change of optical retardation, resulting from the crystallization of PEO, was smaller than the corresponding triblock copolymer. This difference was attributed to the higher crystalline volume ratio ($\phi_{c,PEO}/\phi_{c,PLLA}$) and the enhanced chain orientation of the triblock copolymer. The long period change as a function of temperature was measured by SAXS, and as the temperature increased from 20 to 80 °C, the long period increased by 33% for the triblock copolymer ($\phi_{PLLA} = 0.57$). Together these results indicate that the crystallization of PEO in the triblock copolymer, i.e., the crystallization of PEO with both ends of the chain anchored to the PLLA crystals, is influenced by the presence of the PLLA crystals, causing an enhancement in the relative orientation of the PLLA and PEO crystals. However, in the case of the blend, the orientation of the PEO lamellae confined between the PLLA lamellae is also biased due to the crystallization of the PEO in confined geometry.

Acknowledgment. This work was supported by the U.S. Department of Energy under Contract DE-FG03-88ER45375, the Army Research Laboratory under Contract W911NF-04-1-0191, the NSF-supported Materials Research Science and Engineering Center (DMR-0213695), and the Korean Science Foundation supported Hyperstructured Organic Materials Research Center (HOMRC) at Seoul National University.

References and Notes

(1) Bates, F. S.; Fredrickson, G. H. *Annu. Rev. Phys. Chem.* **1990**, *41*, 525.
(2) Zhu, L.; Cheng, S. Z. D.; Calhoun, B. H.; Ge, Q.; Quirk, R. P.; Thomas, E. L.; Hsiao, B.; Yeh, F.; Lotz, B. *J. Am. Chem. Soc.* **2000**, *122*, 5957.
(3) Albuerne, J.; Marquez, L.; Muller, A. J.; Paquez, J. M.; Degee, P.; Dubois, P.; Castelletto, V.; Hamley, I. W. *Macromolecules* **2003**, *36*, 1633.
(4) Hong, S.; MacKnight, W. J.; Russell, T. P.; Gido, S. P. *Macromolecules* **2001**, *34*, 2398.
(5) Hong, S.; MacKnight, W. J.; Russell, T. P.; Gido, S. P. *Macromolecules* **2001**, *34*, 2878.
(6) Misra, A.; Garg, S. N. *J. Polym. Sci., Polym. Phys.* **1986**, *24*, 983.
(7) Lee, S.-Y.; Chin, I.-J.; Jung, J.-S. *Eur. Polym. J.* **1999**, *35*, 2147.
(8) Choi, Y. K.; Bae, Y. H.; Kim, S. W. *Macromolecules* **1998**, *31*, 8766.
(9) Bogdanov, B.; Vidts, A.; Schacht, E.; Berghmans, H. *Macromolecules* **1999**, *32*, 726.
(10) Wang, Y.; Hillmyer, M. A. *J. Polym. Sci., Polym. Chem.* **2001**, *39*, 2755.
(11) Ho, R.-M.; Hsieh, P.-Y.; Tseng, W.-H.; Lin, C.-C.; Huang, B.-H.; Lotz, B. *Macromolecules* **2003**, *36*, 9085.
(12) Bhattarai, N.; Kim, H. Y.; Cha, D. I.; Lee, D. R.; Yoo, D. I. *Eur. Polym. J.* **2003**, *39*, 1365.
(13) Martin, O.; Averous, L. *Polymer* **2001**, *42*, 6209.
(14) Jeong, B.; Bae, Y. H.; Lee, D. S.; Kim, S. W. *Nature (London)* **1997**, *388*, 860.
(15) Nijenhuis, A. J.; Colstee, E.; Grijpma, D. W.; Pennings, A. J. *Polymer* **1996**, *37*, 5849.
(16) Nakafuku, C.; Sakoda, M. *Polym. J.* **1993**, *25*, 909.
(17) Mark, J. E., Ed. *Polymer Data Handbook*; Oxford University Press: New York, 1999.
(18) Aamer, K.; Sardina, H. A.; Bhatia, S.; Tew, G. N. *Biomaterials* **2004**, *25,* 1087.
(19) Brandrup, J., Imergut, E. H., Eds.; *Polymer Handbook*, 3rd ed.; Wiley-Interscience: New York, 1989.
(20) Hu, Y.; Hu, Y. S.; Topolkaraev, V.; Hiltner, A.; Baer, E. *Polymer* **2003**, *44*, 5681.
(21) Nojima, S.; Wang, D.; Ashida, T. *Polym. J.* **1991**, *23*, 1473.
(22) Keith, H. D.; Padden, F. J., Jr.; Russell, T. P. *Macromolecules* **1989**, *22*, 666.
(23) Stein, R. S. *J. Appl. Phys.* **1961**, *32*, 1280.
(24) Takahashi, Y.; Tadokoro, H. *Macromolecules* **1973**, *6*, 672.
(25) Hoogsteen, W.; Postema, A. R.; Pennings, A. J.; Brinke, G.; Zugenmaier, P. *Macromolecules* **1990**, *23*, 634.
(26) Kokturk, G.; Serhatkulu, T. F.; Cakmak, M.; Piskin, E. *Polym. Eng. Sci.* **2002**, *42*, 1619.
(27) McGowan, J. C. *Polymer* **1969**, *10*, 841.

MA0481712